



Carbon nanotube (CNT) forest grown on diamond-like carbon (DLC) thin films significantly improves electrochemical sensitivity and selectivity towards dopamine



Sami Sainio^a, Tommi Palomäki^a, Sneha Rhode^b, Minna Kauppila^c, Olli Pitkänen^d, Tuula Selkälä^d, Geza Toth^d, Michelle Moram^b, Krisztian Kordas^d, Jari Koskinen^e, Tomi Laurila^{a,*}

^a Department of Electrical Engineering and Automation, School of Electrical Engineering, Aalto University, 02150 Espoo, Finland

^b Department of Materials, Faculty of Engineering, Imperial College, London, UK

^c Department of Applied Physics, School of Science, Aalto University, Finland

^d Department of Electrical Engineering, University of Oulu, Finland

^e Department of Materials Science, School of Chemical Technology, Aalto University, Espoo, Finland

ARTICLE INFO

Article history:

Received 26 August 2014

Received in revised form 5 January 2015

Accepted 7 January 2015

Available online 28 January 2015

Keywords:

Carbon nanotubes
Diamond-like carbon
Electrochemistry
Dopamine
Biomaterials

ABSTRACT

In this study we demonstrate a scalable and CMOS compatible synthesis of robust diamond-like carbon (DLC)–multi-walled carbon nanotube (MWCNT) hybrid electrodes. MWCNTs were grown directly on top of DLC thin film electrodes by utilizing Al/Co/Fe tri-layer catalyst structure at 550 °C. The structure of the hybrid material was characterized in detail by utilizing scanning electron microscopy (SEM), transmission electron microscopy (TEM), Raman investigations and X-ray photoelectron spectroscopy (XPS). After a very simple activation step with nitric acid the material was shown to exhibit a wide stable water window, almost reversible electron transfer kinetics and high sensitivity as well as selectivity towards dopamine (DA) in the presence of ascorbic acid (AA). Thus, it can be argued that the electrochemical properties of DLC and MWCNT were combined in a unique way in this new hybrid nanomaterial. The possible reasons behind the observed behavior are discussed in considerable detail. Despite the fact that present results are valid only for this particular hybrid material synthesized under conditions described in this paper, we anticipate that by utilizing the concept of DLC–MWCNT hybrids, several other novel carbon based electrode materials may be introduced for a wide variety of electrochemical and other applications.

© 2015 Elsevier B.V. All rights reserved.

1. Introduction

It has been estimated that currently up to 27% of the adult population in Europe are affected by mental and neurological disorders [1]. Many of these disorders are directly related to different neurotransmitters, specifically to the amount of neurotransmitters present in different parts of brain [2–5].

Carbon based materials have been frequently used *in vitro* for detecting neurotransmitters [6–9]. Especially, carbon fiber (CF) has been utilized as electrode material. However it is vulnerable to biofouling [6,8], geometries of the electrodes are limited and it is not compatible with standard silicon processes. Recently, promising results have been achieved by using diamond-like carbon (DLC) [10] coated electrodes [11–13]. DLC possess many favorable

properties such as stability, good biocompatibility [14–17] and resistance to bacterial adhesion [18,19]. These sensors have been successfully used to detect 10 μM concentrations of dopamine (DA) [11,12], which means that they are not sensitive enough to detect the required levels of dopamine *in vivo*, which, depending on the measurement techniques and location, vary between 5 and 700 nM [20–22]. In addition, when dopamine is measured in the presence of interfering elements, such as ascorbic acid, which are present *in vivo* with much higher concentrations than dopamine, the analysis of the latter becomes very difficult. This is because the interfering substances typically oxidize approximately at the same potential as DA. As it is known that CNTs may exhibit fast electron transfer rates [23,24], it can be hypothesized that if CNTs can be grown directly on top of high sp³ containing DLC substrates at low enough temperatures, a stable corrosion resistant, biocompatible, patternable, CMOS compatible and electrochemically active hybrid material could be fabricated.

* Corresponding author. Tel.: +358 503414375.
E-mail address: tomi.laurila@aalto.fi (T. Laurila).

Carbon nanotube films and forests have found use in electrode applications for many years. When directly growing the nanotubes on conductive surfaces, electrical interfacing becomes straightforward due to the intimate contact at the substrate–CNT interface. This has been exploited for example in electrochemical double-layer capacitors [25,26], batteries [23,27] and field emitter devices [24]. The relatively large amount of nanotubes that can be synthesized directly on a given substrate ($\sim 30 \text{ mg/cm}^2$ for forests of 1 mm thickness [28]) allows substantially large effective electrode areas of $\sim 1.5 \text{ m}^2/\text{cm}^2$ (assuming a specific surface area of $\sim 50 \text{ m}^2/\text{g}$ for CVD grown CNTs [29]) and thus enhances electrochemical sensitivity compared to very thin films deposited typically by drop-casting or by electrophoresis. A further advantage of the directly grown nanotube films is their structural integrity and mechanical robustness enabling more reliable operation than that using physisorbed nanotubes e.g. on glassy carbon surfaces.

Although the combination of DLC with other nanostructured carbons as a novel family of carbon based hybrid materials has been recognized lately [30–33] and its excellent optical absorbance was shown to be useful in solar energy harvesting [31], the expectedly fascinating electrochemical sensing characteristics have not been explored yet.

In this paper, we report a scalable and CMOS compatible synthesis method to grow robust diamond-like carbon and carbon nanotube hybrid structures by the means of cathodic arc and subsequent chemical vapor deposition. We also demonstrate how these hybrid materials can be used for electrochemical sensing to detect and quantify dopamine (DA) in solutions in the presence of interfering elements. The developed hybrid carbon based electrodes show a wide and stable water window and almost reversible electron transfer kinetics allowing efficient electrochemical analysis of dopamine with detection limit of less than 500 nM. In addition, it is shown that the hybrid electrodes are capable of readily distinguishing ascorbic acid and dopamine oxidation peaks making the electrodes promising candidates for biochemical applications.

2. Experimental

The substrate materials used for the diamond-like carbon (DLC) thin films were n-type Si (100) wafers (Okmetic). The wafers were etched in buffered HF solution and dried in flowing nitrogen right before the deposition. The deposition chamber of 70 L volume was pumped with an oil diffusion pump to a base pressure of 1×10^{-3} Pa. The samples were mounted by hanging in a rotating carousel (0.04 rpm) with planetary rotation of the substrate holders. The chamber has two arc sources and one ion source on the chamber walls. Prior to deposition, the samples were etched by using a griddles argon ion source and coated with Ti using a continuous current arc source equipped with 60° magnetic filtering. The arc current used was 55 A and the duration of the deposition was 35 s. The role of Ti is to ensure excellent adhesion of the DLC layer on the substrate. For the carbon a 2.6 mF capacitor bank was charged to 200 V and the arc was triggered with ignition electrodes. The maximum pulse current was 3 kA and the pulse half width was about 150 μs . Each pulse was triggered separately at 1 Hz frequency. The deposition rate during the pulse was 1.4×10^{15} ions/ cm^2 , as measured from the growth rate of a carbon layer on a flat silicon substrate. The distance from the cathode varied between 150 and 300 mm during the deposition due to sample rotation. The average carbon ion energy has been previously measured to be 40–50 eV using an electrostatic probe. It may be assumed that all carbon in the plasma is ionized.

Carbon nanotube films were grown on the DLC layers by the means of catalytic vapor deposition (CVD) from acetylene precursor

similar to our previous report [34]. In brief, multilayer catalyst films of Al (0.2 nm), Co (3 nm), Fe (3 nm) were deposited by e-beam and thermal evaporation methods on the DLC films prior MWCNT growth. The deposition rates of the metals were monitored with a quartz crystal balance. The catalyst coated substrates were inserted to a cold wall CVD reactor (Aixtron, Black Magic, UK) and heated to the process temperatures (550°C) using an electrically heated holder to reduce the catalyst metals in NH_3 at 250 sccm flow rate and 10 mbar pressure for 10 min. In the next step, the reactor chamber was evacuated to a base pressure of 0.2 mbar, and then filled with N_2 buffer (250 sccm) while setting and maintaining a reactor pressure of 10 mbar. After the pressure was stabilized, C_2H_2 (carbon precursor, 25 sccm) was introduced into the chamber. The growth phase took 10 min in each experiment.

The hybrid materials were pretreated with nitric acid (68% concentration), by submerging the electrode to the acid for 5 min. After the activation of the electrode surface, edges and backside were covered with protective PTFE-film (Saint-Gobain Performance Plastics CHR 2255-2). Hole with a diameter of 8 mm was made to the film before placing it on the electrode surface, to allow the solution to reach contact with the electrode.

Cyclic voltammetry (CV) was carried out with Gamry Reference 600 Potentiostat/Galvanostat/ZRA. Water window was measured in 0.15 M sulfuric acid and the dopamine measurements utilized different concentrations of dopamine in phosphate buffered saline (PBS) solution. A 10 mM dopamine solution was prepared, by using dopamine hydrochloride (Sigma–Aldrich, St. Louis, USA), in phosphate-buffered saline (PBS Dulbecco, Biochrom AG, Berlin, Germany) that was further diluted to obtain a series of dopamine solutions from a concentration of 1 mM–1 nM. Sweep rate was typically set to 50 mV/s. The reference electrode was Ag/AgCl skinny reference electrode provided by Sarissa Biomedical Ltd, pH values of the H_2SO_4 and PBS solutions were, 0.55 and 7.4, respectively. All the solutions were deoxygenated with N_2 for 5 min prior to measurement and the air in the electrochemical cell was purged with N_2 during the measurements. All the measurements were conducted at room temperature. Ferrocenemethanol (FcMeOH) (Sigma–Aldrich, St. Louis, USA) was used as an outer-sphere redox system to define the electron transfer rate of the electrode. The measurements were conducted in 1 mM FcMeOH solution in 0.15 M sulfuric acid (Merck kGaA, Darmstadt, Germany). The measurements were carried out at scan rates of 10, 50, 100, 200 and 400 mV/s.

X-ray photoelectron spectroscopy was carried out with SSX-100 ESCA under ultra-high vacuum using Al K_α radiation (1486.6 eV). The surface topography of the hybrid carbon coated sensing layers were assessed by scanning electron microscopy (JEOL JSM-6330F and Zeiss Ultra plus) as well as by transmission electron microscopy (EFTEM, Leo 912 Omega, 120 kV). Cross-sectional TEM samples were prepared conventionally by grinding, polishing and dimpling the specimen until its thickness was below 10 microns, followed by Ar ion milling performed using a PIPS Ion miller (Gatan USA). High-resolution transmission electron microscopy (HRTEM) was performed using a double-aberration-corrected JEOL 2100 (JEOL, Japan) microscope equipped with a field emission gun (FEG) operating at 200 kV. Moreover, the JEOL 2100 microscope was used to perform scanning transmission electron microscopy (STEM) using high angle annular dark-field (HAADF) imaging. The JEOL 2100 was equipped with the Gatan image filter (GIF) for electron energy-loss spectroscopy (EELS). A Gatan $4k \times 4k$ UltraScan 4000 CCD camera was employed for digital recording of the HRTEM images. Raman spectra of the pristine DLC and CNT on DLC films were recorded using a Horiba Jobin-Yvon Labram HR800 UV-VIS micro-Raman equipment.

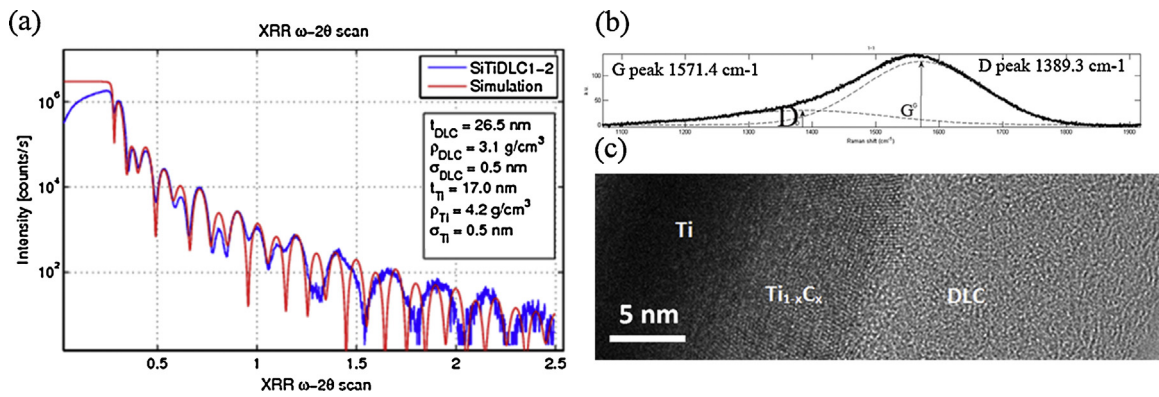


Fig. 1. (a) XRR, (b) and (c) TEM analyses for the DLC thin film substrates.

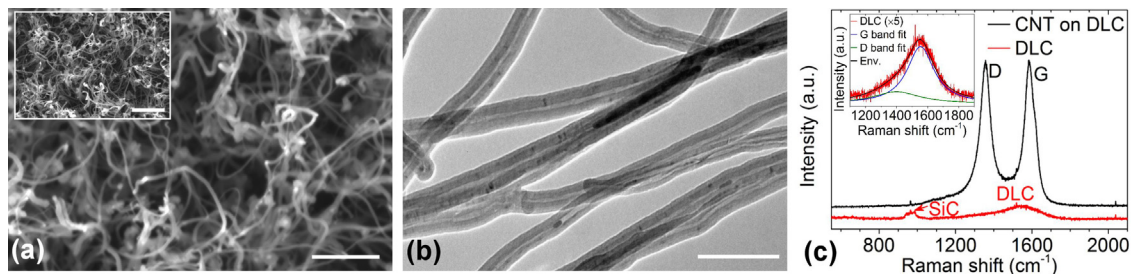


Fig. 2. (a) Scanning and (b) transmission electron micrographs of carbon nanotubes grown on diamond-like carbon surfaces. The scale bars are 1 μm (inset), 500 nm (panel a) and 100 nm (panel b). (c) Corresponding Raman spectra of the substrate and the hybrid structure. The inset shows a magnified (5 \times) and base line corrected fit of the Raman D and G bands centering at 1554 cm^{-1} and 1400 cm^{-1} and with a peak ratio $I_D/I_G \sim 1$.

3. Results and discussion

The DLC thin films used as the substrates for the CNT growth had a mass density of about 3.1 g/cm^3 as determined previously with X-ray reflectivity (XRR) measurements, which together with the Raman analyses indicate a high sp^3 content (about 75–80%) (Fig. 1(a) and (b)). [12] In addition, the DLC films were practically hydrogen free. The thickness of the DLC layers used in the electrodes was about 20 nm and that of the underlying Ti adhesion layer about 30 nm. It should be observed that in the XRR measurements about 30 nm thick DLC layers were used for analysis purposes. Based on the cross-sectional transmission electron microscope (TEM) investigations the layers were of uniform thickness and the structure of the DLC was amorphous without any visible crystalline areas (Fig. 1 (c)). More details about the DLC thin films can be found from [12].

Continuous films of multi-walled carbon nanotubes (diameter of 20–40 nm) emerge on the diamond-like carbon surfaces shortly after the start of the growth period as indicated by the darkened and optically diffuse surface. Electron microscopy analysis revealed that the nanotube films on the surface were only partially aligned, and the nanotubes were slightly curved (Fig. 2(a)–(c)). This can be explained by the relatively low growth temperature ($550\text{ }^\circ\text{C}$) and associated higher defect density in the nanotube

walls than in those usually obtained under optimized conditions at $\sim 700\text{--}800\text{ }^\circ\text{C}$. Raman spectroscopy also supports the large defect density ($I_D/I_G \sim 1.0$) in the nanotubes (Fig. 1(c)). On the other hand, the low growth temperature used makes the current growth process CMOS compatible. The length of the nanotubes is somewhat less than $10\text{ }\mu\text{m}$ after 10 min synthesis as expected at $550\text{ }^\circ\text{C}$ in agreement with our earlier results showing the bulk diffusion of carbon atoms in the catalyst is the major limiting factor when growing nanotubes on Co-Fe bimetallic catalyst from acetylene precursor [34]. Variations in the MWCNT film density may be observed for some of the samples depending on the synthesis batch because of unevenness in the DLC and/or catalyst layers under the nanotubes. It is important to point out that in our experiments the layer thickness of Al (0.2 nm) is considerably lower than the typically applied optimum of 10–15 nm in order to avoid a complete blockage of the DLC layer and yet ensuring a sufficient barrier to avoid diffusion and subsequent poisoning of the catalyst in the DLC film underneath.

Cross-sectional TEM analysis was carried out next to investigate what has taken place during the growth of the MWCNTs on top of DLC. The micrographs are shown in Fig. 3. From the STEM-HAADF data in Fig. 3(a) one can identify the Si and DLC+MWCNT owing to the similar contrast in the STEM-HAADF image. The Ti layer

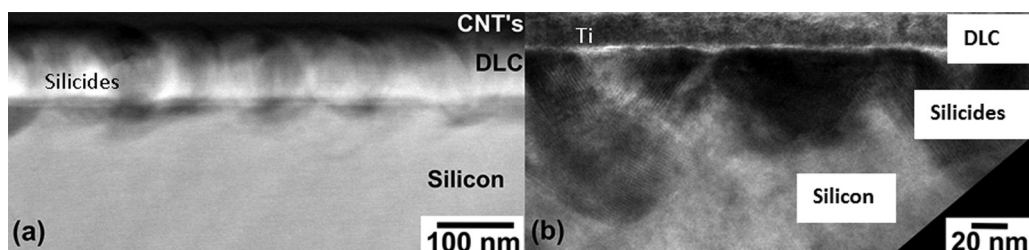


Fig. 3. (a) Cross-sectional STEM-HAADF image and (b) cross-sectional multi-beam HRTEM image along the zone axis of the MWCNT on DLC film.

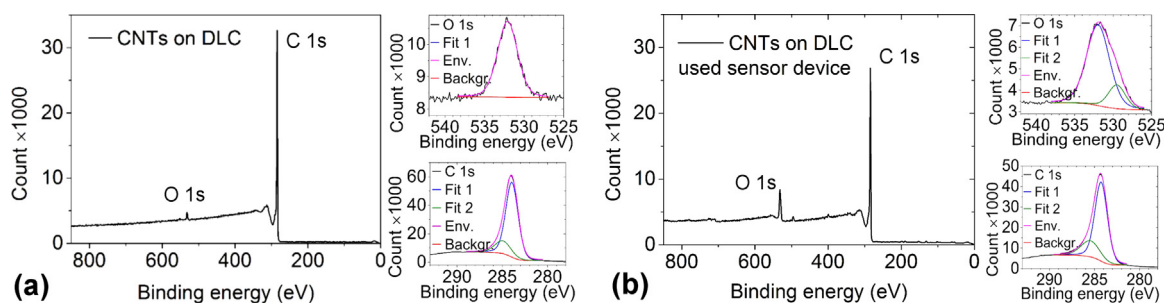


Fig. 4. X-ray photoelectron spectra (survey, O 1s and C 1s) of MWCNTs on DLC hybrid sensor structures (a) before and (b) after use.

can be identified between the Si and DLC because of the brighter appearance than the neighboring Si and DLC layers. There are also darker 'triangular' regions at the Si/Ti interface, which appear to be small voids, which are often seen at interfaces with Si. Inside the DLC+MWCNT "layer" one can see several bright areas, which correspond most likely to phases containing metallic elements, such as (Fe,Co)-silicides and Fe-Co particles formed during the activation of the catalyst and the growth of the nanotubes. From the HRTEM data shown in Fig. 3(b) one can identify Si at the bottom of the image, the 'void' regions in the middle and the interface between the Si and the next layer at the top. This layer is polycrystalline as we can see from the fringes and is therefore the Ti adhesion layer. On top of that starts the DLC+MWCNT "layer". The DLC layer also appears to be partly graphitized. Thus, based on what has been stated above it appears that the catalysts have reacted with the Si during the growth of MWCNTs, as expected based on the thermal load to which the samples have been subjected during the synthesis. In addition, the voids probably contain also some silicide(s), because we can see fringes with different orientations in the HRTEM images and this definitely does not come from the Si alone. However the voids are not 100% filled with silicide because if they would, they would look bright, instead of dark, in Fig. 3(a). It is to be noted that all metallic elements, excluding Al, can react with Si to form various silicides as already discussed above. Unfortunately, owing to the small dimensions of the "silicide" areas it is not possible to obtain a proper quantitative analysis of their composition. However, EDX analyses indicate that they contain Fe, Co and Si as expected. A more detailed TEM investigation of the interfacial structure will be reported elsewhere [35].

To investigate the surface chemistry of the samples X-ray photoelectron spectroscopy analysis was carried out. The results from the as-deposited heterostructures revealed only traces of Co (778.6 eV) and FeO (709.9 eV), whereas no Al or its oxidized species were found in the spectrum. The asymmetric C 1s peak is similar to those reported for CNTs with a main C–C peak at 294.0 eV, and lower energy satellites (e.g. due to C–O) as well as the characteristic broad peak of the delocalized electrons around 291 eV were also observed. The symmetrically positioned O 1s peak at 531.7 eV indicates the presence of OH-groups on the surface as shown in Fig. 4(a). Based on the XPS analyses, there were hardly any differences in the peaks of oxygen, cobalt or iron between the unused and activated samples. However once the electrode has been used, a shoulder at 529.2 eV appears due to metal oxides that most probably originate from the partially dissolved and re-deposited catalyst (in the form of oxide) during the cyclic voltammetry measurements. The presence of low intensity peaks at 710.8 eV and 781.2 eV also support the presence of oxides/hydroxides of both Fe and Co, respectively. The SEM micrographs (Fig. 5) taken from the unused, activated and used samples also show that there are no significant structural differences between the electrodes. It is also seen that the alignment of the CNTs is not exactly vertical but they are more or less randomly oriented. This can again be understood based on the low growth

temperature and resulting high defect density. In conclusion, based on the above analyses it can be stated that the hybrid CNT+DLC material is relatively robust and does not degrade markedly in use.

From Fig. 6(a) it is evident that the water window of the hybrid carbon material is relatively wide (about 2.7 V). In fact, it is not significantly narrower in comparison to that of the plain tetrahedral amorphous carbon (ta-C) DLC (about 3.4 V). The threshold current used here to determine the water window limits was 200 μ A. The capacitances of the electrical double layers of the two materials were calculated based on the data from 50 mV/s and 400 mV/s cyclic voltammograms. Geometric area of the corresponding electrode was used and the difference between the anodic and cathodic current densities was used ($\Delta i = 2 \times C \times v$). The resulting values are higher in the case of hybrid carbon material ($349 \pm 87 \mu\text{F}/\text{cm}^2$) when compared to the plain DLC ($62.2 \pm 18.6 \mu\text{F}/\text{cm}^2$). However, if one takes into account the approximated increase in the surface area of the DLC+CNT electrode (at least ~ 50 times) the "reduced" double layer capacitance (calculated at 0 V vs. Ag/AgCl at 400 mV/s) of the hybrid electrode ($\sim 7 \pm 1.8 \mu\text{F}/\text{cm}^2$) is actually smaller than that of plain DLC. It should, however, be noted that there is no clear double layer region in the voltammogram shown in Fig. 6(a). This indicates that most likely some faradic reactions take place at the surface of the electrodes and therefore the capacitance values obtained include also a "pseudocapacitance" part in addition to the actual double layer value. In fact, based on the XPS analyses discussed above there are at least –OH groups (and most likely also –COOH groups) present on top of the electrode surfaces after processing. It is anticipated that these groups will participate the faradic reactions contributing to the measured pseudocapacitance. One can also note that the hybrid carbon electrode is stable while in contact with H_2SO_4 as there are practically no changes in the cyclic voltammograms between the 1st and 20th cycle.

The results of the FcMeOH measurements are shown in Fig. 6(b). It can be seen that in this case there are actually two peaks present in the voltammogram with the hybrid carbon material instead of one peak, which is expected based on the one electron transfer reaction and outer sphere nature of FcMeOH. The larger peak is attributed to MWCNTs and the smaller peak to the substrate, since the latter one is approximately at the same location as the FcMeOH peak for the plain DLC sample (Fig. 6(b)). This points out that the CNTs do not completely cover the underlying surface. The peak currents associated with the oxidation and reduction reactions are significantly higher in the case of the hybrid material, as expected based on the higher surface area. The peak separations for the FcMeOH reaction on CNT and on DLC are given in Table 1 along with the heterogeneous electrochemical constants k_e calculated by utilizing Eq. (1)

$$\psi = \frac{\gamma^\alpha k_e}{\sqrt{(\pi a D_0)}} \quad (1)$$

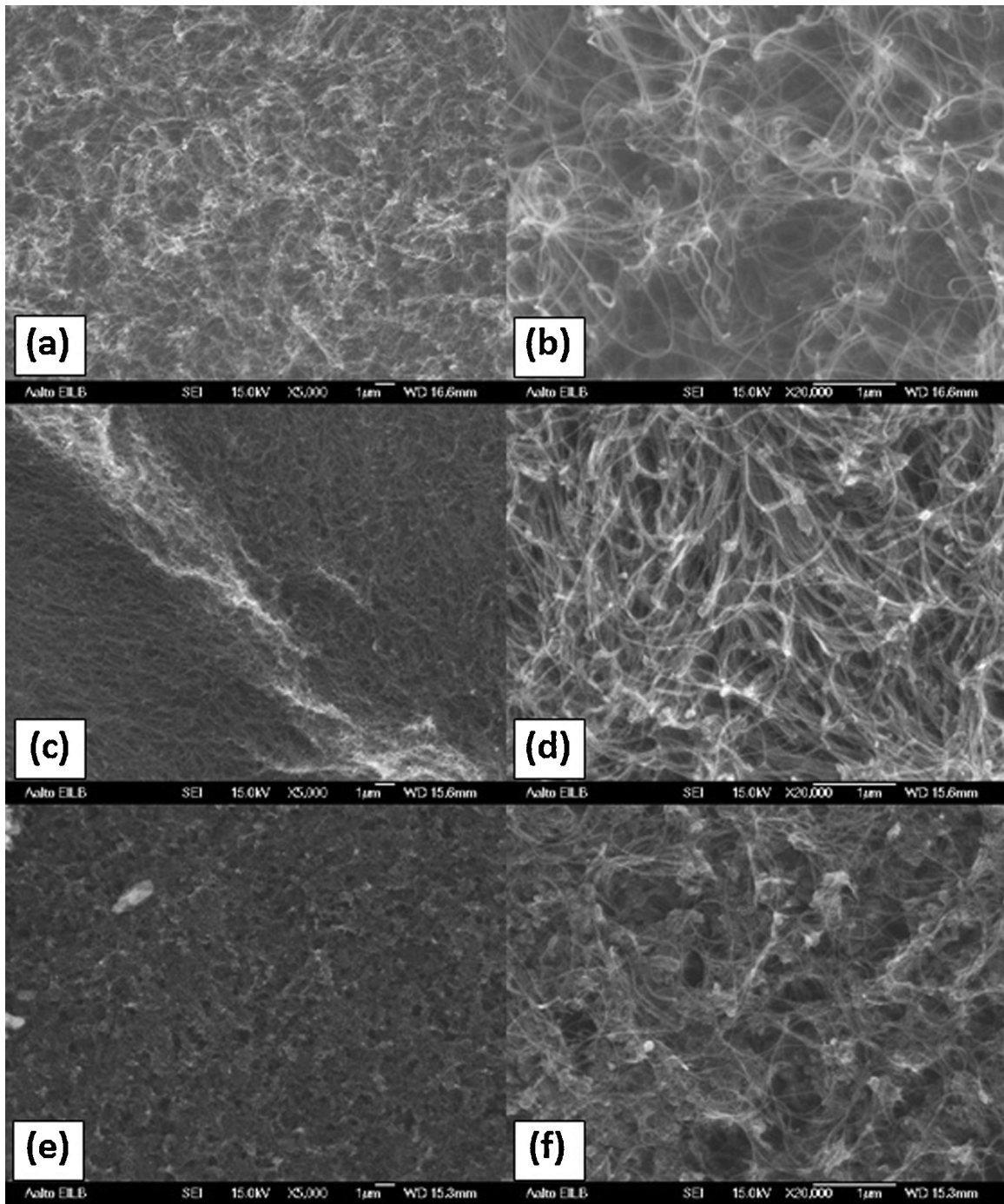


Fig. 5. Scanning electron micrographs of MWCNTs on DLC (a, b) before and (c, d) after activation as well as (e, f) after use in electrochemical measurements.

given by Nicholson in [36] at 298 K, taking diffusion coefficient (D_{Fc}) of ferrocene to be $2.17 \times 10^{-5} \text{ cm}^2/\text{s}$ [37] (same value for both oxidized and reduced form). γ is the square root of the ratio of the diffusion coefficients of the oxidized and reduced forms of the

molecule in question, $a = nFv/RT$ (n is the number of electrons transferred, F is the Faradays constant 96,485 C/mol, R is the universal gas constant 8.314 J/kmol and v is the cycling speed in V/s and T is temperature in K) and charge transfer coefficient α has been

Table 1

Table shows the oxidation peak positions of ferrocenemethanol on DLC and hybrid MWCNT on DLC electrodes using different voltage scan rates and the calculated heterogeneous electrochemical rate constants. Detection limits of dopamine on DLC and hybrid MWCNT on DLC electrodes are also shown together with the peak separations.

Electrode	Water window (200 μA threshold)	Double layer pseudo-capacitance ($\mu\text{F}/\text{cm}^2$)	ΔE_p (FcMeOH) (50 mV/s)	ΔE_p (FcMeOH) (400 mV/s)	k_e (cm/s) (FcMeOH)	Detection limit (DA) (50 mV/s)	ΔE_p (DA) (50 mV/s)
DLC + CNT	2.7 V	349 ± 87	62 mV	72 mV	0.15	500 nM	22 mV
DLC	3.4 V	62.2 ± 18.6	220 mV	352 mV	7.8×10^{-4}	10 μM	448 mV

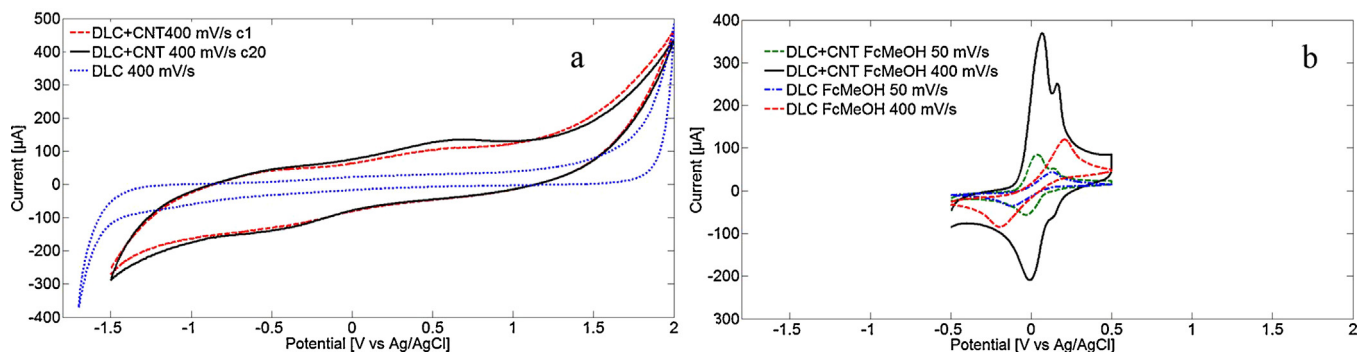


Fig. 6. Cyclic voltammetry analyses of (a) the water window and (b) ferrocenemethanol oxidation for both DLC and MWCNT on DLC hybrid electrodes in 0.15 M H₂SO₄.

taken as 0.5. Values of ψ as a function of peak potential difference observed in the CV curve were taken from [36]. Based on the results it is evident that there is apparently a very large difference in the electron transfer properties between the hybrid carbon material and plain DLC. In fact, the heterogeneous electron transfer coefficient is among the highest values obtained with CNT containing electrodes [38,39], but at the same time double layer capacitance ($349 \pm 87 \mu\text{F}/\text{cm}^2$) is much smaller than reported with other high performance CNT electrodes [38]. However, caution must be taken when the calculated heterogeneous electron transfer coefficient for the hybrid electrode material is considered. (i) Firstly, as shown in [40,41] the presence of porous layer on top of a planar electrode will significantly alter the diffusion behavior of the reactive element, as there will be a marked contribution from thin layer diffusion. Thus, one cannot directly compare the heterogeneous reaction constants calculated for the DLC and DLC + MWCNT electrodes, as the mass transport regimes in the two cases are most likely different. In fact, the sharp appearance of the oxidation and reduction peaks in the case of hybrid DLC + MWCNT material implicate that there is significant contribution from the thin surface layer present on top of the electrode. (ii) Secondly, the treatment based on the Nicholson method can give us only an idea how the heterogeneous reaction constant changes from that of plain DLC to that of DLC + MWCNT, as it will most likely not give correct results for the present thin layer case, where the boundary conditions for diffusion are different from the semi-infinite system on which the treatment is based on [36,42,43]. As a matter of fact, in [40,41] it has been shown by simulation that in cases where there is considerable contribution from thin layer diffusion, the peak separation is a function of diffusion layer thickness while k_e is kept constant. Thus, this will directly influence the heterogeneous reaction constant calculated by the Nicholson method. Therefore, the value given in Table 1 should be used only to support the idea that the MWCNT forest on top of DLC thin film electrode markedly increases the electron transfer rate in this particular case. With respect to the last statement it must also be emphasized that any changes in the density, defect population and length or diameter of the MWCNTs will change also the electrochemical response. Thus, the results obtained here are relevant only for the present hybrid DLC + MWCNT material.

Sensitivity of the electrodes towards dopamine (Fig. 7(a) and (b)) shows that concentrations down to 500 nM of DA can be detected with the hybrid carbon sensor whereas the plain DLC can detect only 10 μM . It should be noted that no background subtraction has been used here and the data shown in Fig. 7 is not manipulated in anyway, but represents the true raw measurement results. Thus, it is the opinion of the authors that these direct measurement results are much more important in quantifying the performance of the electrode than the calculated values presented below and typically shown in the literature. To assess the reproducibility of the

measurements some of them were repeated with the same electrode several times. While doing this no significant changes in the response were detected. More detailed discussion about the stability of the electrodes is given below. Thus, sensitivity and stability of the hybrid material falls within the range required under physiological conditions. The peaks associated with DA oxidation and reduction at 10 μM concentration in the DLC + MWCNT hybrid are situated at about 98 mV and 72 mV, respectively, whereas those for plain DLC at 100 μM are at about 404 mV and -44 mV (all vs. Ag/AgCl). The reason for using different concentrations in the peak separation comparison is that in the case of DLC there was no reduction peak visible at 10 μM concentration. Thus, the better electron transfer properties implicated by the FcMeOH measurements are reflected also as higher sensitivity towards DA. While comparing the response of the two types of electrode materials to dopamine following observations can be made: (i) The peak positions are more easily attributable owing to the better defined shape of the peaks in the case of DLC + MWCNT hybrid. (ii) Concentrations down to 500 nM show distinct peaks with DLC + MWCNT hybrid whereas with DLC alone there is hardly any peak at 10 μM , but instead a step-like increase in current followed by a shoulder is observed. (iii) More importantly, the peak separation is much smaller with the DLC + MWCNT hybrid material (Fig. 7(a) and (b)), which indicates that the heterogeneous electrochemical reaction constant (contributing to peak positions) of the hybrid material may be considerably higher than that of plain DLC. In fact, the observed peak separation in the case of the hybrid material is smaller than the value corresponding to reversible two electron redox process (which is 29.5 mV). However, as discussed above, these results may be interpreted based on the relatively high contribution of thin layer diffusion of species entrapped within the porous-like layer to diffusional mass transport regime, as suggested in [40,41]. Thus, again direct comparison between the peak separation values between DLC and DLC + MWCNT electrodes should not be carried out as the mass transfer regimes in the case of the two electrodes are most likely different. Again the presence of thin layer contribution is supported by the sharp peaks for oxidation in the case of DLC + CNT electrode. In fact, when DA concentration is 10 μM the diffusive tail of the oxidation peak on top of the hybrid electrode is still evident, but for more dilute solutions the peak is more “thin layer-like”. However, as discussed below the electrochemical behavior of the present system may well be even more complicated as preferential adsorption of DA on the DLC + MWCNT electrodes may also take place. The oxidation currents for dopamine scale approximately linearly as a function of concentration with the DLC + CNT electrode in the concentration range of interest (500 nM–10 μM) ($I (\mu\text{A}) = 0.27 (\mu\text{M}) + 0.84 (R^2 = 0.9909)$). The limit of detection (LOD) and limit of quantification (LOQ) were calculated according to the procedure given in [44–46] (i.e. LOD was taken as $3.3 \times \sigma/S$, where σ is the standard deviation of the background signal and S the sensitivity,

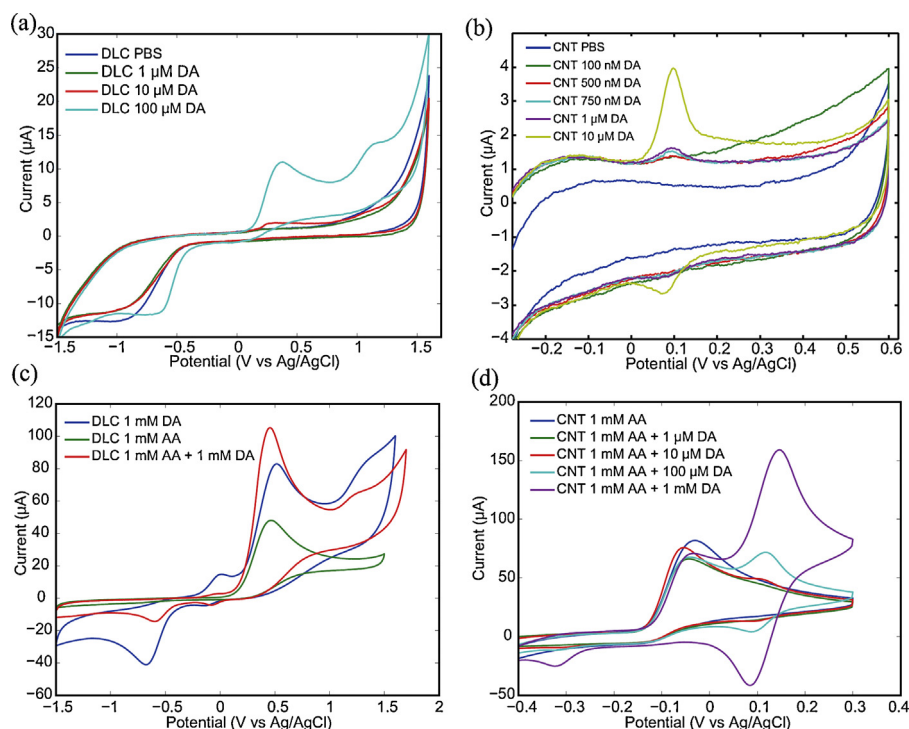


Fig. 7. Cyclic voltammetry analyses of (a) DLC and (b) MWCNT on DLC hybrid sensor response towards dopamine at cycling speed of 50 mV/s. Measurements done in the presence of ascorbic acid are shown for (c) DLC and (d) DLC + MWCNT hybrid.

and the LOQ as $10 \times \sigma/S$. Based on the estimation the sensitivity is $1138 \mu\text{A}/\text{mM}$, LOD is $1.26 \pm 0.23 \text{ nM}$ and LOQ $3.8 \pm 0.84 \text{ nM}$. These values are among the best reported in the literature for dopamine detection (references [46–51] and Table 2). Thus, the new material shows great potential to be used in biodetection application, especially as our results are from CV measurements and not from more sensitive differential pulse voltammetry (DPV) measurements.

While considering the results from FcMeOH, which is a simple outer sphere redox couple and dopamine, it should be noted that DA is known to show complex adsorption behavior on top of many electrode materials whereas FcMeOH is free of such complications [52]. Therefore, one should not draw too strong of a conclusion

based on the different peak values and further investigations of the DA reactions must be carried out. The oxygen functionalities of the MWCNTs as observed with XPS will be deprotonated at physiological pH to a large extent, thus yielding a negative overall surface charge for the CNT network. Thus, this may influence the adsorption behavior of DA, which is cationic at physiological pH. This would also influence the peak shape by making it more symmetric and by reducing peak separation, if adsorption is enhanced. Further, the oxidation of catechols is known to be a two-electron, two-proton transfer process in which the hydroquinone oxidizes to orthoquinone. In this sequence the order of proton and electron transfer follows a scheme of squares and is dependent

Table 2

Results from the literature showing different investigations about the sensitivity and selectivity of different electrode materials towards dopamine in the presence of various interfering elements.

Ref.	Year	Electrode material	Detection method	DA (μM)	AA (μM)	HT-5 (μM)	UA (μM)
[63]	2013	CNF	DPV	0.1–10	1000	0.25–10	x
[64]	2006	CF	ACV (+Hilbert Transform)	5	500	1	x
[65]	2014	SDS-MWCNTs/GCE	DPV	1–100	400–3500	x	4–30
[66]	2011	DNA/PAMAM/MWNP	DPV	4–200	1000	x	20–1000
[67]	2013	Pt NPs on polydopamine coated CNTs	DPV CV	0.5–20 50	x 1000	x x	0.6–13 50
[68]	2002	CNT modified graphite	DPV	0.5–8	80–1360	x	x
[69]	2003	PDMA coated GC	Square wave voltammetry	1.2–36	200	x	x
[70]	1995	Acetonitrile modified GC	DPV	20	2000	x	x
[71]	2006	Poly(3,4-ethylenedioxy) thiophene modified GC	Square wave voltammetry	20–60	200	x	x

DPV = differential pulse voltammetry, CV = cyclic voltammetry, ACV = AC voltammetry, DA = dopamine, AA = ascorbic acid, HT-5 = serotonin, UA = uric acid.

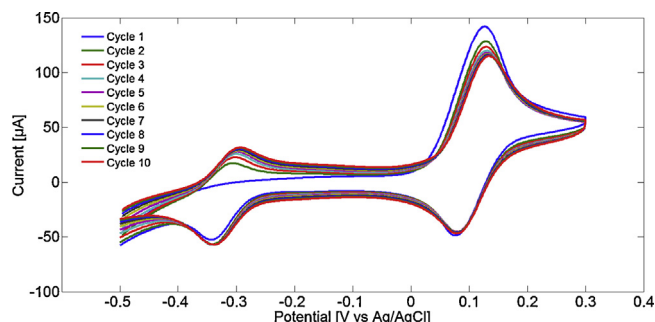


Fig. 8. Cyclic voltammogram showing the behavior of DLC+MWCNT electrode when cycled ten times in 1 mM solution of dopamine at cycling speed of 50 mV/s.

on pH [53,54]. The surface charge of the substrate can also influence the order of this process. The proposed transfer sequence for catechols is H^+ , e^- , H^+ , e^- on carbon paste, glassy carbon and platinum electrodes at neutral pH [53,54]. In fact, we have recently carried out a detailed investigation about the effects of pH on the catechol, methylcatechol and DA reactions on different carbon electrodes and the results indeed show a very strong pH dependency [55].

As it was discussed in the introduction, it is of utmost importance for a feasible electrode material to be able to distinguish between dopamine and common interfering elements, such as ascorbic acid (AA), present *in vivo* with much higher concentrations than dopamine [56–61]. In Fig. 7(c) and (d) CV results from the dopamine measurements in the presence of ascorbic acid are shown. When one compares the performance of the hybrid DLC + CNT material to the plain DLC electrode it is evident that when dopamine and ascorbic acid are present at the same time DLC cannot resolve between them whereas the hybrid DLC + CNT is capable of differentiating between the two (Fig. 7(c) and (d)). When there is two orders of magnitude larger concentration of AA than DA the peaks are still clearly resolved. However, typical ratio of AA to DA is from 1000 to 10,000, depending on the location of the brain [59,62]. Therefore, more work is needed to improve the selectivity and sensitivity of this hybrid material to achieve higher AA to DA ratios. In Table 2 several results from the selectivity investigations from the literature are shown. As one can see, there are results that show higher ratio for AA to DA than the present investigations. However, these have been determined with differential pulse voltammetry (DPV) which is in general superior to CV in sensitivity and selectivity [43]. In fact, if one takes from Table 2 the only investigation carried out with CV the ratio of AA to DA in that investigation is smaller than in this paper. Thus, one can therefore conclude that the results obtained so far are encouraging, since by utilizing for example DPV with this material would most likely result into considerable higher sensitivities and selectivities. Finally, when one considers interfering elements one should also take into account 3,4-dihydroxyphenylacetic acid (DOPAC), which is a metabolite of dopamine. DOPAC is a likely candidate as an interfering element in the *in vivo* measurements, when measuring DA, as its oxidation peak is expected to be at the same potential as the DA's oxidation peak. Based on research in [71,72] DA levels are clearly lower than DOPAC levels in striatum, and measurements of DA carried out in [71] were not actually measuring DA, but actually DOPAC. Therefore, more investigation of DA vs. DOPAC measurements needs to be conducted with these hybrid sensors.

Another important issue related to the possible *in vivo* use is the fouling of the electrode surfaces. It has been recently shown that DLC electrodes suffer from this phenomenon especially when wide potential windows are used with DA concentrations in the mM range [73]. In the case of DLC + CNT hybrid electrodes similar behavior was not seen even when a wide potential window was

used (Fig. 8) One can see that there is a slight decrease in the peak current after continuous cycling, but no significant change in the peak position or complete passivation, as observed with DLC alone [73]. The other peaks seen at lower potentials in Fig. 8 are related to leucodopaminechrome (LDAC) and dopaminechrome (DAC) as shown in [73]. In addition, when a narrow potential window is used, which is feasible as the peak separation between DA oxidation and reduction is very small in this case, even less fouling is seen even after tens of cycles.

4. Conclusions

In summary, a new electrochemical sensing platform based on a hybrid carbon material has been introduced in this work. The new material combines the properties of the high sp^3 containing diamond-like carbon with those of carbon nanotubes, and takes the electrochemical performance of this new material beyond those of its individual components. The CNTs were grown directly on top of thin film DLC electrodes by CVD process. After a very simple activation process, the new electrodes were shown to exhibit a wide stable water window, reasonably low “reduced” double layer capacitance, facile electron transfer kinetics and high sensitivity as well as selectivity towards dopamine. The low temperature and short growth times applied in the synthesis of hybrid DLC–CNT devices make the fabrication process CMOS compatible as well as scalable. Further, SEM (Figs. 2 and 5) and XPS (Fig. 4) analyses showed that there were hardly any changes at the surfaces of the samples after activation or measurement, thus indicating relative robustness of the new electrode material. With further optimization of the structures (e.g. CNT network density or pretreatments) we expect reliable DA detection down to few nM concentration ranges and in the presence of interfering elements, such as ascorbic acid. Even though the results presented here are valid only for the specific DLC + CNT hybrid synthesized in this investigation, it can be expected that the demonstrated new hybrid carbon materials can pave the road for a new family of carbon based electrochemical sensing electrodes suitable for diverse applications.

Acknowledgements

The authors S.S., T.P., J.K. and T.L. would like to acknowledge the National Agency for Technology and Innovation (grant number 211488) and Aalto University for financial support

References

- [1] H.U. Wittchen, F. Jacobi, J. Rehm, A. Gustavsson, M. Svensson, B. Jönsson, J. Olesen, C. Allgulander, J. Alonso, C. Faravelli, L. Fratiglioni, P. Jennum, R. Lieb, A. Maercker, J. van Os, M. Preisig, L. Salvador-Carulla, R. Simon, H.C. Steinhausen, Cost of disorders of the brain in Europe 2010, *Eur. Neuropsychopharm.* 21 (2011) 655–679.
- [2] M.F. Bear, B.W. Connors, M.A. Paradiso, *Neuroscience Exploring the Brain*, 3rd ed., Lippincott Williams & Wilkins, Philadelphia, 2007, 837.
- [3] M.J. Hurley, P. Jenner, What has been learnt from study of dopamine receptors in Parkinson's disease? *Pharmacol. Ther.* 111 (2006) 715–728.
- [4] N.D. Volkow, G.-J. Wang, S.H. Kollins, T.L. Wigal, J.H. Newcorn, F. Telang, J.S. Fowler, W. Zhu, J. Logan, Y. Ma, K. Pradhan, C. Wong, J.M. Swanson, Evaluating dopamine reward pathway in ADHD, *JAMA: J. Am. Med. Assoc.* 302 (2009) 1084–1091.
- [5] A. Frisch, E. Michaelovsky, R. Rockah, I. Amir, H. Hermesh, N. Laor, C. Fuchs, J. Zohar, B. Lerer, S.F. Buniak, S. Landa, M. Poyurovsky, B. Shapira, R. Weizman, Association between obsessive-compulsive disorder and polymorphisms of genes encoding components of the serotonergic and dopaminergic pathways, *Eur. Neuropsychopharm.* 10 (2000) 205–209.
- [6] C.A. Anastassiou, B.A. Patel, M. Arundell, M.S. Yeoman, K.H. Parker, D. O'Hare, Subsecond voltammetric separation between dopamine and serotonin in the presence of ascorbate, *Anal. Chem.* 78 (2006) 6990–6998.
- [7] P.S. Cahill, Q.D. Walker, J.M. Finnegan, G.E. Mickelson, E.R. Travis, R.M. Wightman, Microelectrodes for the measurement of catecholamines in biological systems, *Anal. Chem.* 68 (1996) 3180–3186.
- [8] P. Takmakov, M.K. Zachek, R.B. Keithley, P.L. Walsh, C. Donley, G.S. McCarty, R.M. Wightman, Carbon microelectrodes with a renewable surface, *Anal. Chem.* 82 (2010) 2020–2028.

- [9] S.H. DuVall, R.L. McCreery, Control of catechol and hydroquinone electron-transfer kinetics on native and modified glassy carbon electrodes, *Anal. Chem.* 71 (1999) 4594–4602.
- [10] J. Robertson, Diamond-like amorphous carbon, *Mater. Sci. Eng. R* 37 (2002) 129–281.
- [11] E. Kaivosoja, S. Sainio, J. Lyytinen, T. Palomäki, T. Laurila, I.S. Kim, J.G. Han, J. Koskinen, Carbon thin films as electrode material in neural sensing, *Surf. Coat. Technol.* 259 (2014) 33–38, <http://dx.doi.org/10.1016/j.surfcoat.2014.07.056>.
- [12] T. Laurila, A. Rautiainen, S. Sintonen, H. Jiang, E. Kaivosoja, J. Koskinen, Diamond-like carbon (DLC) thin film bioelectrodes: effect of thermal post treatments and the use of Ti adhesion layer, *Mater. Sci. Eng. C* 34 (2014) 446–454.
- [13] E. Kaivosoja, E. Berg, A. Rautiainen, T. Palomäki, J. Koskinen, M. Paulasto-Kröckel, T. Laurila, Improving the function of dopamine electrodes with novel carbon materials, *Conf. Proc. IEEE Eng. Med. Biol. Soc.* (2013) 632–634, <http://dx.doi.org/10.1109/EMBC.2013.6609579>.
- [14] M. Allen, B. Myer, N. Rushto, In vitro and in vivo investigations into the biocompatibility of diamond-like carbon (DLC) coatings for orthopedic applications, *J. Biomed. Mater. Res.* 58 (2001) 319–328.
- [15] E. Kaivosoja, S. Myllymaa, Y. Takakubo, H. Korhonen, K. Myllymaa, Y.T. Konttinen, R. Lappalainen, M. Takagi, Osteogenesis of human mesenchymal stem cells on micro-patterned surfaces, *J. Biomater. Appl.* 27 (2013) 862–871.
- [16] E. Kaivosoja, P. Suvanto, G. Barreto, S. Aura, A. Soininen, S. Franssila, Y.T. Konttinen, Cell adhesion and osteogenic differentiation on three-dimensional pillar surfaces, *J. Biomed. Mater. Res. A* 101 (2013) 842–852.
- [17] S. Myllymaa, E. Kaivosoja, K. Myllymaa, T. Sillat, H. Korhonen, R. Lappalainen, Y.T. Konttinen, Adhesion, spreading and osteogenic differentiation of mesenchymal stem cells cultured on micropatterned amorphous diamond, titanium, tantalum and chromium coatings on silicon, *J. Mater. Sci. Mater. Med.* 21 (2010) 329–341.
- [18] K. Myllymaa, J. Levon, V.-M. Tiainen, S. Myllymaa, A. Soininen, H. Korhonen, E. Kaivosoja, R. Lappalainen, Y.T. Konttinen, Formation and retention of staphylococcal biofilms on DLC and its hybrids compared to metals used as biomaterials, *Colloid Surf. B* 101 (2013) 290–297.
- [19] A. Soininen, V.-M. Tiainen, Y.T. Konttinen, H. van der Mei, H.J. Busscher, P.K. Sharma, Bacterial adhesion to diamond-like carbon as compared to stainless steel, *J. Biomed. Mater. Res. A* 90 (2009) 882–885.
- [20] J.B. Venton, M.R. Wightman, Psychoanalytical electrochemistry: dopamine and behaviour, *Anal. Chem.* 75 (2003) 414–421.
- [21] M.L.A.V. Heien, A.S. Khan, J.L. Ariansen, J.F. Cheer, P.E.M. Phillips, K.M. Wasum, R.M. Wightman, Real-time measurements of dopamine fluctuations after cocaine in the brain of behaving rats, *Proc. Natl. Acad. Sci. U.S.A.* 102 (2005) 10023–10028.
- [22] D.L. Robinson, J.B. Venton, M.L.A.V. Heien, M.R. Wightman, Detecting subsecond dopamine release with fast-scan cyclic voltammetry in vivo, *Clin. Chem.* 49 (2003) 1763–1773.
- [23] C.E. Banks, T.J. Davies, G.G. Wildgoose, R.G. Compton, Electrocatalysis at graphite and carbon nanotube modified electrodes: edge-plane sites and tube ends are the reactive sites, *Chem. Commun.* (2005) 829–841.
- [24] J.J. Gooding, Nanostructuring electrodes with carbon nanotubes: a review on electrochemistry and applications for sensing, *Electrochim. Acta* 50 (2005) 3049–3060.
- [25] N. Halonen, J. Mäklän, A.-R. Rautio, J. Kukkola, A. Uusimäki, G. Toth, L.M. Reddy, R. Vajtai, P.M. Ajayan, K. Kordas, Thin micropatterned multi-walled carbon nanotube films for electrodes, *Chem. Phys. Lett.* 583 (2013) 87–91.
- [26] S. Talapatra, S. Kar, S.K. Pal, R. Vajtai, L. Ci, P. Victor, M.M. Shaijumon, S. Kaur, O. Nalamasu, P.M. Ajayan, Direct growth of aligned carbon nanotubes on bulk metals, *Nat. Nanotechnol.* 1 (2006) 112–116.
- [27] S. Sridhar, L. Ge, C.S. Tiwary, A.C. Hart, S. Ozden, K. Kalaga, S. Lei, S.V. Sridhar, R.K. Sinha, H. Harsh, K. Kordas, P.M. Ajayan, R. Vajtai, Enhanced field emission properties from CNT arrays synthesized on inconel superalloy, *ACS Appl. Mater. Interfaces* 6 (2014) 1986–1991.
- [28] N. Halonen, K. Kordas, G. Toth, T. Mustonen, J. Mäklän, J. Vähäkangas, P.M. Ajayan, R. Vajtai, Controlled CCVD synthesis of robust multiwalled carbon nanotube films, *J. Phys. Chem. C* 112 (2008) 6723–6728.
- [29] N. Halonen, A. Rautio, A.-R. Leino, T. Kyllönen, G. Toth, J. Lappalainen, K. Kordas, M. Huuhtanen, R.L. Keiski, A. Sapi, M. Szabo, A. Kukovec, Z. Konya, I. Kiricsi, P.M. Ajayan, R. Vajtai, Three-dimensional carbon nanotube scaffolds as particulate filters and catalyst support membranes, *ACS Nano* 4 (2010) 2003–2008.
- [30] C. Wei, C.-I. Wang, F.-C. Tai, K. Ting, R.-C. Chang, The effect of CNT content on the surface and mechanical properties of CNTs doped diamond like carbon films, *Diamond Relat. Mater.* 19 (2010) 562–566.
- [31] N.T. Panagiotopoulos, E.K. Diamanti, L.E. Koutsokeras, M. Baikousi, E. Kordatos, T.E. Matikas, D. Gournis, P. Patsalas, Nanocomposite catalysts producing durable, super-black carbon nanotube systems: applications in solar thermal harvesting, *ACS Nano* 6 (2012) 10475–10485.
- [32] E.C. Choi, Y.S. Park, B. Hong, Synthesis of carbon nanotubes on diamond-like carbon by the hot filament plasma-enhanced chemical vapor deposition method, *Micron* 40 (2009) 612–616.
- [33] R. Cartwright, S. Esconjauregui, D. Hardeman, S. Bhardwaj, R. Weatherup, Y. Guo, L. D'Arise, B. Bayer, P. Kidambi, S. Hofmann, E. Wright, J. Clarke, D. Oakes, C. Cepek, J. Robertson, Low temperature growth of carbon nanotubes on tetrahedral amorphous carbon using Fe-Cu catalyst, *Carbon* 81 (2015) 639–649.
- [34] O. Pitkänen, N. Halonen, A.-R. Leino, J. Mäklän, A. Dombovari, J.H. Lin, G. Toth, K. Kordas, Low-temperature growth of carbon nanotubes on bi- and tri-metallic catalyst templates, *Top. Catal.* 56 (2013) 522–526.
- [35] T. Laurila, H. Jiang, S. Sainio, O. Pitkänen, K. Kordas, J. Koskinen, Multi-walled Carbon Nanotubes (MWCNTs) grown directly on tetrahedral amorphous carbon (ta-C): an detailed transmission electron microscopy (TEM) interfacial study, (submitted for publication).
- [36] R. Nicholson, Theory and application of cyclic voltammetry for measurement of electrode reaction kinetics, *Anal. Chem.* 37 (1965) 1351–1355.
- [37] J. Baur, R. Wightman, Diffusion coefficients determined with microelectrodes, *J. Electroanal. Chem.* 305 (1991) 73–81.
- [38] P. Papakonstantinou, R. Kern, L. Robinson, H. Murphy, J. Irvine, E. McAdams, J. McLaughlin, T. McNally, Fundamental electrochemical properties of carbon nanotube electrodes, *Carbon Nanostruct.* 13 (2005) 91–108.
- [39] F. Valentini, A. Amine, S. Orlanducci, M.L. Terranova, G. Palleschi, Carbon nanotube purification: preparation and characterization of carbon nanotube paste electrodes, *Anal. Chem.* 75 (2005) 5413–5421.
- [40] I. Streeter, G.G. Wildgoose, L. Shao, R.G. Compton, Cyclic voltammetry on electrode surfaces covered with porous layers: An analysis of electron transfer kinetics at single-walled carbon nanotube modified electrodes, *Sens. Actuators B* 133 (2008) 462–466.
- [41] G.P. Keeley, M.E.G. Lyons, The effects of thin layer diffusion at glassy carbon electrodes modified with porous films of single-walled carbon nanotubes, *Int. J. Electrochem. Sci.* 4 (2009) 794–809.
- [42] R. Compton, G. Banks, *Understanding Voltammetry*, 2nd ed., Imperial College Press, 2010, pp. 444.
- [43] A. Bard, L. Faulkner, *Electrochemical Methods: Fundamentals and Applications*, 2nd ed., Wiley, 2001, pp. 833.
- [44] A. Gutierrez, M. Lozano, L. Galicia, N. Ferreyra, G. Rivas, Electrochemical sensing of uric acid using glassy carbon modified with multiwall carbon nanotubes dispersed in polyethylenimine, *Electroanalysis* 26 (2014) 2191–2196.
- [45] A. Gasnier, J. Gonzalez-Dominguez, A. Anson-Casaos, J. Hernandez-Ferrer, M. Pedano, M. Rubianes, M. Martinez, G. Rivas, Single-wall carbon nanotubes covalently functionalized with polylysine: synthesis, characterization and analytical applications for the development of electrochemical (bio)sensors, *Electroanalysis* 26 (2014) 1676–1683.
- [46] F. Gutierrez, F. Comba, A. Gasnier, A. Gutierrez, L. Galicia, C. Parrado, M. Rubianes, G. Rivas, Graphene paste electrode: analytical applications for the quantification of dopamine, phenolic compounds and ethanol, *Electroanalysis* 26 (2014) 1694–1701.
- [47] Z. Wang, J. Xia, L. Zhu, X. Chen, F. Zhang, S. Yao, Y. Li, Y. Xia, A selective voltammetric method for detecting dopamine at quercetin modified electrode incorporating graphene, *Electroanalysis* 23 (2011) 2463–2471.
- [48] M. Zhu, C. Zeng, J. Ye, Graphene-modified carbon fiber microelectrode for the detection of dopamine in mice hippocampus tissue, *Electroanalysis* 23 (2011) 907–914.
- [49] P. Si, H. Chen, P. Kannan, D.-H. Kim, Selective and sensitive determination of dopamine by composites of polypyrrole and graphene modified electrodes, *Analyst* 136 (2011) 5134–5138.
- [50] L. Wu, L. Feng, J. Ren, X. Qu, Electrochemical detection of dopamine using porphyrin-functionalized graphene, *Biosens. Bioelectron.* 34 (2012) 57–62.
- [51] S. Hon, M.L. Kasner, S. Su, K. Patel, R. Cuellari, Highly sensitive and selective dopamine biosensor fabricated with silanized graphene, *J. Phys. Chem. C* 114 (2010) 14915–14921.
- [52] S. Chumillas, M. Figueiredo, V. Climent, J. Feliu, Study of dopamine reactivity on platinum single crystal electrode surfaces, *Electrochem. Acta* 109 (2013) 577–586.
- [53] M.R. Deakin, P.M. Kovach, K.J. Stutts, R.M. Wightman, Heterogeneous mechanisms of the oxidation of catechols and ascorbic acid at carbon electrodes, *Anal. Chem.* 58 (1986) 1474–1480.
- [54] E. Laviron, Electrochemical reactions with protonations at equilibrium: part X. The kinetics of the p-benzoquinone/hydroquinone couple on a platinum electrode, *J. Electroanal. Chem.* 164 (1984) 213–227.
- [55] T. Palomäki, S. Chumillas, S. Sainio, V. Prototopova, J. Koskinen, V. Climent, J.M. Feliu, T. Laurila, Dopamine and quinone redox reactions at diamond-like carbon thin film electrodes, (submitted for publication).
- [56] J.J. Burmeister, G.A. Gerhardt, Ceramic-based multisite microelectrode arrays for in vivo electrochemical recordings of glutamate and other neurochemicals, *TrAC Trends Anal. Chem.* 22 (2003) 498–502.
- [57] J.M. Cooper, P.L. Foreman, A. Glidle, T.W. Ling, D.J. Pritchard, Glutamate oxidase enzyme electrodes: microsensors for neurotransmitter determination using electrochemically polymerized permselective films, *J. Electroanal. Chem.* 388 (1995) 143–149.
- [58] M.A. Rahman, N.-H. Kwon, M.-S. Won, E.S. Choe, Y.-B. Shim, Functionalized conducting polymer as an enzyme-immobilizing substrate: an amperometric glutamate microbiosensor for in vivo measurements, *Anal. Chem.* 77 (2005) 4854–4860.
- [59] D.L. Robinson, A. Hermans, A.T. Seipel, R.M. Wightman, Monitoring rapid chemical communication in the brain, *Chem. Rev.* 108 (2008) 2554–2584.
- [60] J.O. Schenk, E. Miller, R. Gaddis, R.N. Adams, Homeostatic control of ascorbate concentration in CNS extracellular fluid, *Brain Res.* 253 (1982) 353–356.
- [61] R.D. O'Neill, The measurement of brain ascorbate in vivo and its link with excitatory amino acid neurotransmission, in: A. Boulton, G. Baker, R.N. Adams (Eds.), *Voltammetric Methods in Brain Systems*, Humana Press Inc., 1995, pp. 221–268.
- [62] J.A. Stamford, J.B. Justice Jr., Peer reviewed probing brain chemistry: voltammetry comes of age voltammetry has been solving the mysteries of the brain and its functions for 21 years, *Anal. Chem.* 68 (1996), 359A–363A.

- [63] E. Rand, A. Periyakaruppan, Z. Tanaka, D.A. Zhang, M.P. Marsh, R.J. Andrews, K.H. Lee, B. Chen, M. Meyyappan, J.E. Koehne, A carbon nanofiber based biosensor for simultaneous detection of dopamine and serotonin in the presence of ascorbic acid, *Biosens. Bioelectron.* 42 (2013) 434–438.
- [64] J. Zhang, Z. Zhu, J. Zhu, K. Li, S. Hua, Selective determination of dopamine, ascorbic acid and uric acid at SDS-MWCNTs modified glassy carbon electrode, *Int. J. Electrochem. Sci.* 9 (2014) 1264–1272.
- [65] X. Liua, Y. Penga, X. Qua, S. Aia, R. Hana, X. Zhu, Multi-walled carbon nanotube-chitosan/poly(amidoamine)/DNA nanocomposite modified gold electrode for determination of dopamine and uric acid under coexistence of ascorbic acid, *J. Electroanal. Chem.* 654 (2011) 72–78.
- [66] M. Lin, H. Huang, Y. Liu, C. Liang, S. Fei, X. Chen, C. Ni, High loading of uniformly dispersed Pt nanoparticles on polydopamine coated carbon nanotubes and its application in simultaneous determination of dopamine and uric acid, *Nanotechnology* 24 (2013) 1–9.
- [67] Z. Wang, J. Liu, Q. Liang, Y. Wang, G. Luo, Carbon nanotube-modified electrodes for the simultaneous determination of dopamine and ascorbic acid, *Analyst* 127 (2002) 653–658.
- [68] P.R. Roy, T. Okajima, T. Ohsaka, Simultaneous electroanalysis of dopamine and ascorbic acid using poly (N,N-dimethylaniline)-modified electrodes, *Bioelectrochemistry* 59 (2003) 11–19.
- [69] A.J. Downard, A.D. Roddick, A.M. Bond, Covalent modification of carbon electrodes for voltammetric differentiation of dopamine and ascorbic acid, *Anal. Chim. Acta* 317 (1995) 303–310.
- [70] V.S. Vasantha, S.-M. Chen, Electrocatalysis and simultaneous detection of dopamine and ascorbic acid using poly(3,4-ethylenedioxy)thiophene film modified electrodes, *J. Electroanal. Chem.* 592 (2006) 77–87.
- [71] F. Gonon, M. Buda, R. Cespluglio, M. Jouviet, J.-F. Pujol, In vivo electrochemical detection of catechols in the neostriatum of anaesthetized rats: dopamine or DOPAC? *Nature* 286 (1980) 902–904.
- [72] F.G. Gonon, C.M. Fombarlet, M.J. Buda, J.F. Pujol, Electrochemical treatment of pyrolytic carbon fiber electrodes, *Anal. Chem.* 53 (1981) 1386–1389.
- [73] T. Laurila, V. Protopopova, S. Rhode, S. Sainio, T. Palomäki, M. Moram, J. Feliu, J. Koskinen, New electrochemically improved tetrahedral amorphous carbon films for biosensor applications, *Diamond Relat. Mater.* 49 (2014) 62–71.

Biographies

Mr. Sami Sainio received his MSc from Aalto University on 2013. He is currently pursuing his PhD in the field of hybrid carbon nanomaterials under supervision of Prof. Tomi Laurila.

Mr. Tommi Palomäki received his MSc from Aalto University on 2013. He is currently pursuing his PhD in the field of electrochemistry of carbon nanomaterials under supervision of Prof. Tomi Laurila.

Dr. Sneha Rhode is a Post Doc in the Imperial College London and working as a TEM specialist.

Ms. Minna Kauppila is a research assistant in the Department of Applied Physics in Aalto University.

Mr. Olli Pitkänen is currently pursuing his PhD in the field of carbon nanomaterials at the University of Oulu under supervision of Prof. Krisztian Kordas.

Ms. Tuula Selkälä is working as a staff scientist and microscopist at University of Oulu.

Dr. Geza Toth is a Post Doc at University of Oulu working on the synthesis of CNTs.

Professor Michelle Moram is a Royal Society University Research Fellow and leads the Functional Nitrides group in the Department of Materials at Imperial College which currently includes 4 PDRAs, 12 PhDs and 2 MEng students.

Dr. Krisztian Kordas is a Research Professor at Microelectronics and Materials Physics Laboratories Department of Electrical Engineering at University of Oulu.

Dr. Jari Koskinen is a Professor at Aalto University, School of Chemical Technology.

Dr. Tomi Laurila is an Associate Professor of Microsystem Technology at Aalto University, School of Electrical Engineering.